THE JOURNAL OF PHYSICAL CHEMISTRY A

Article

Cite This: J. Phys. Chem. A 2019, 123, 5692−5703

pubs.acs.org/JPCA

Kinetic Investigations of the CH ($X^2\Pi$) Radical Reaction with Cyclopentadiene

Published as part of The Journal of Physical Chemistry virtual special issue "Pacific Conference on Spectroscopy and Dynamics".

Kacee L. Caster,[†] Zachery N. Donnellan,[†] Talitha M. Selby,[‡] and F. Goulay*[,†]

[†]C. Eugene Bennett Department of Chemistry, West Virginia University, Morgantown, West Virginia 26506, United States

[‡]Department of Mathematics and Natural Sciences, University of Wisconsin—Milwaukee, West Bend, Wisconsin 53095, United States

Supporting Information

ABSTRACT: The reaction of the ground state methylidyne radical (CH ($X^2\Pi$)) with cyclopentadiene (C_5H_6) is studied in a quasi-static reaction cell at pressures ranging from 2.7 to 9.7 Torr and temperatures ranging from 298 to 450 K. The CH radical is generated in the reaction cell by pulsed-laser photolysis (PLP) of gaseous bromoform at 266 nm, and its concentration monitored using laser-induced fluorescence (LIF) with an excitation wavelength of 430.8 nm. The reaction rate coefficient is measured to be 2.70(±1.34) × 10^{-10} cm^3 $molecule^{-1}$ s^{-1} at room temperature and 5.3 Torr and found to be independent of pressure or temperature over the studied experimental ranges. DFT and CBS-QB3 methods are used to calculate the reaction potential energy surface (PES) and to provide insight into the entrance channel of the reaction. The combination of the experimentally determined rate constants and computed PES supports a fast, barrierless entrance channel that is characteristic of CH radical reactions and could potentially lead to the formation of benzene isomers.

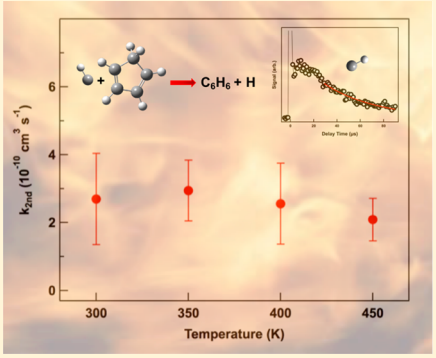

1. INTRODUCTION

Polycyclic aromatic hydrocarbons (PAHs) are known to be molecular precursors to carbon nanoparticles in carbon-rich environments, such as combustion flames,[1,2] planetary atmospheres,[3] and the interstellar medium.[4−7] In combustion processes, PAHs aggregate to form soot, which is a known carcinogen and pollutant.[1,2,8] Their formation is initiated during the pyrolysis and oxidation of fuel molecules through reactions with free radicals such as OH, O atom, C_2H, and CH. These radicals propagate complex chemical schemes leading to the first aromatic ring and eventually to peri-condensed aromatic rings. Commonly accepted PAH growth schemes center on repetitive reactions and include the well-known HACA (Hydrogen-Abstraction-C_2H_2-Addition) mechanism.[2,9,10] This mechanism proceeds by sequential hydrogen abstraction from an aromatic molecule followed by acetylene addition to the subsequent radical site. Similar mechanisms replacing acetylene with methyl, propargyl, and cyclopentadienyl radicals also lead to the formation of large PAHs.[11−15] The significance of the various pathways is largely dependent on the structure of the fuel molecule and the reaction conditions.[16] In addition, the formation of the first ring is generally regarded as the main rate-limiting step in the overall molecular growth scheme and has been widely studied.[2,17,18] The predictive capability of models focusing on replicating the complexity of combustion environments is limited by the lack of kinetic and thermodynamic data about an extensive number of reactions under relevant conditions, especially the formation of benzene and first peri-condensed aromatic rings.

Cyclopentadiene (CPD, C_5H_6) is an abundant conjugated combustion intermediate that has been shown to play a central role during the formation of aromatic molecules[19−22] It has been detected during the pyrolysis of toluene ($C_6H_5CH_3$) and benzyl radical ($C_6H_5CH_2$).[23,24] The oxidation of benzene has also been shown to produce significant amounts of cyclopentadiene over the 300−1000 K temperature range.[25] More recently, CPD has been identified as a major product during the pyrolysis of the jet fuel JP-10 with branching fractions greater than 15% reported over the 1300−1600 K temperature range.[26] These product fractions are in good agreement with prior experimental studies conducted over a wide range of temperatures and pressures, suggesting CPD as a major product.[19,27−30] Vandewiele et al.[19] examined the secondary reaction products of JP-10 pyrolysis and found that CPD was the central first ring involved in the formation of PAHs such as naphthalene and indene. Theoretical models also suggest that the addition of the cyclopentadienyl radical to the neutral CPD molecule provides additional routes to naphthalene and

Received: April 23, 2019
Revised: June 4, 2019
Published: June 13, 2019

DOI: 10.1021/acs.jpca.9b03813
J. Phys. Chem. A 2019, 123, 5692−5703

indene.[31] Further reaction of the formed PAHs with CPD could yield fluorenes, which are larger three- and four-ring PAH structures with five-membered ring constituents.[21] The presence of five-membered rings in PAHs has been shown to facilitate isomerization and dimerization in these molecules and to effectively contribute to higher sooting tendencies during combustion processes.[32,33] Although CPD is an important combustion intermediate during PAH formation, its reactions with reactive combustion intermediates has largely been overlooked.

The importance of small free radical species for the formation of PAHs in combustion environments has been long established.[1,8,15,18,34] One of the most reactive radical species in combustion environments is the methylidyne (CH) radical. This radical is unique in structure due to a singly occupied and a vacant nonbonding molecular orbital centralized on the carbon atom, in addition to a filled orbital that also lends a carbene-like nature.[35] The reaction mechanisms of the CH radical with unsaturated hydrocarbons involve little to no barrier, leading to reactions proceeding at a fraction of the collision rate. The initial encounter of the reactants is followed immediately by the formation of an initial, short-lived intermediate that isomerizes and decomposes to give the final products. These initial short-lived intermediates are typically formed through either CH insertion into a C—H σ-bond or through cycloaddition across the C=C π-system of the reacting molecule. There is a great deal of evidence to support these CH radical entrance channels, which can be summarized in a general chemical scheme described by a CH-addition/insertion-H-elimination mechanism: CH + C_nH_m → $C_{n+1}H_m$ + H.[36−38] General CH radical mechanisms suggest that the reaction is more likely to proceed through a singlet-carbene-like cycloaddition across the π-system of the molecule to form a three-membered ring constituent.[35] This initial intermediate may rapidly ring open or isomerize and further dissociate through hydrogen elimination to form the final products. In the absence of π-bonds, as in the case of the CH reaction with CH_4,[39−42] the measured rate coefficients still remain fast and support a barrierless CH insertion into the sigma C−H bonds of the molecule. Recent investigations into the products of the CH + pyrrole (C_4H_4NH) reaction by Soorkia et al.[43] strongly support the cycloaddition pathway as the dominate channel. The authors propose a four-step ring expansion pathway following the general CH mechanism that results in the formation of six-membered pyridine (C_5H_5N) + H. The occurrence of π-bonds in the structure of the initial reactant lends preference to the cycloaddition entrance channel over the insertion entrance channel mechanism.[35,36]

The reaction rate of CH radicals with unsaturated hydrocarbons have been extensively studied over the past few decades.[36,38,40,41,44−48] Canosa et al.[40] studied the experimental rate coefficients for CH reactions with ethylene (C_2H_4) and butene (C_4H_8) over a temperature range of 23 to 295 K using pulsed-laser photolysis (PLP) and laser-induced fluorescence (LIF) to probe the radical decay. At 295 K, rate coefficients of $k_{C_2H_4}$ = 2.92(±0.22) × 10^{-10} cm^{-3} $molecule^{-1}$ s^{-1} and $k_{C_4H_8}$ = 3.70(±0.25) × 10^{-10} cm^{-3} $molecule^{-1}$ s^{-1} were reported. Fast and pressure-independent rate coefficients were observed down to 23 K. The rate coefficients displayed a slight positive temperature dependence from 23 K up to 75 K, where a maximum was reached, after which a negative temperature dependence dominated up to 295 K. This negative temperature dependence is consistent with a rapid, barrierless CH addition mechanism, as proposed by Butler et al.[49] in their study of CH + C_2H_4. Canosa and co-workers[40] also suggested that the kinetics below room temperature is governed by long-range electrostatic forces between the reactants.

Berman et al.[45] measured rate coefficients using pump−probe laser techniques at room temperature for the reactions with ethylene ($k_{C_2H_4}$ = 4.2(±0.3) × 10^{-10} cm^{-3} $molecule^{-1}$ s^{-1}), benzene ($k_{C_6H_6}$ = 4.3(±0.2) × 10^{-10} cm^{-3} $molecule^{-1}$ s^{-1}), and toluene ($k_{C_6H_5CH_3}$ = 5.0(±0.4) × 10^{-10} cm^{-3} $molecule^{-1}$ s^{-1}). In the case of ethylene, the rate coefficients displayed a negative temperature dependence over a temperature range of 160 to 652 K. For the CH + benzene reaction, the rate coefficient was found to be independent of temperature over the 297 to 674 K range,[45] although the authors were unable to conclude with certainty on this result due to systematic error from photodissociation of benzene in the reaction cell. Goulay et al.[50] studied the reaction of CH with anthracene ($C_{14}H_{10}$) and reported similar collision-limit rate coefficients with a slight positive temperature dependence over the 58−470 K temperature range. On the mechanistic evidence discussed above and the rapid reactions with unsaturated molecules, the CH radical is likely to be capable of facilitating molecular growth and possibly ring expansion in cyclic unsaturated hydrocarbons in the gas phase. Its reaction with conjugated cyclic molecules, such as CPD, could play a major role during the PAH-growth rate-limiting first ring formation step. The accurate measurement of the rate coefficients for such reactions contributes to improving the accuracy of combustion models.

The present study provides experimentally determined rate coefficients for the reaction of the CH($X^2\Pi$) radical with cyclopentadiene over the 298−450 K temperature range. Part of the C_6H_7 potential energy surface is calculated using B3LYP and CBS-QB3 levels of theory and discussed in conjunction with the experimental kinetics in order to better understand the reaction mechanism. A portion of the C_6H_7 surface has been previously discussed for the study of fulvene to benzene H-assisted isomerization,[51,52] although no previous studies reveal direct information on the entrance channel for the title reaction. Here, the potential energy surface of the two most likely CH radical reaction entrance pathways are predominantly investigated: CH cycloaddition across a C=C bond and CH insertion into one of the C—H bonds of cyclopentadiene. Barrier calculations for both reaction entrance channels are attempted but none are located on the surface within the employed level of theory. The experimental data support the fact that if any barriers to the formation of the initial intermediates exist, they are likely small and submerged, and thus can be considered negligible.[35,48] Additionally, the products for H abstraction pathways and the potential formation of several C_6H_6 species are explored and discussed.

2. EXPERIMENTAL PROCEDURE

2.1. Experimental Setup. A detailed description of the experimental setup for the kinetic measurements has been given elsewhere[53] and only a brief overview is presented here. The kinetic measurements are conducted in a pressure-regulated, heatable, six-way cross stainless-steel reaction cell. The pressure is regulated from approximately 2−10 Torr using a manual butterfly valve while the temperature is varied from 298 to 450 K through the use of heating tape. A retractable

DOI: 10.1021/acs.jpca.9b03813
J. Phys. Chem. A 2019, 123, 5692−5703

Type K thermocouple placed close to the laser-overlap region of the reaction cell is used to monitor and regulate the gas temperature. The four horizontal Brewster-angle ports of the reaction cell are used for laser access while a vertical port supports the photomultiplier tube (PMT). All gases are introduced using calibrated mass flow controllers into a preheated 50 cm^3 mixing volume before introduction in the reaction cell. The deposition of bromoform and cyclopentadiene onto the entrance laser window is mitigated by flowing of a small quantity (~3% of the total flow) of nitrogen gas adjacent to the window's surface.

Bromoform (Sigma-Aldrich, 99%) is photolyzed at 266 nm using the fourth harmonic of a Nd:YAG laser, generating CH radicals in their ground ($X^2\Pi$) and first excited ($A^2\Delta$) electronic states. A small flow of nitrogen (<5% of the total flow) is introduced to quench the vibrationally excited CH($X^2\Pi$, ν = 1) state formed during the photolysis of the precursor.[54] The excited electronic CH($A^2\Delta$), formed by successive three photon photolysis, is identifiable by a strong emission signal immediately after photolysis and rapidly decaying within 3 μs.[55,56] The formed ground state radicals of interest are excited on the $A^2\Delta(\nu = 0) \leftarrow X^2\Pi(\nu = 0)$ vibronic band at 430.8 nm using a 355 nm pumped dye laser with Stilbene 420 dye (Exciton). The LIF signal of the CH radical from the $A^2\Delta(\nu = 0) \rightarrow X^2\Pi(\nu = 1)$ vibronic band is collected by the PMT through a 490 nm (fwhm ±10 nm) band-pass filter. The collected fluorescence is integrated over a 1.1 μs gate, 500 ns after the probe laser pulse and averaged (SRS 250 Boxcar Integrator). Relative radical number density temporal profiles are obtained by changing the delay time between the pump/probe lasers using a delay generator (SRS DG535) with 1 μs delay steps and averaging 10 laser shots per point. The temporal profiles are fit using an exponential decay from 30 to 100 μs after the pump laser pulse. Earlier times are not included in the fit in order to avoid any effect from the N_2-collisional relaxation of the CH ($X^2\Pi$, v = 1) radicals. The experiments are repeated for various concentrations of cyclopentadiene to obtain the second-order rate coefficient at a given pressure and temperature.

Cyclopentadiene reactant is prepared through thermal cracking of its dimer dicyclopentadiene and collection of the distillate in a liquid nitrogen cold trap.[57] A detailed description of the synthesis is provided in the Supporting Information. The sample is degassed and vacuum transferred to a collection cylinder and stored in a total of 1000 Torr of argon buffer gas. The molar fraction of cyclopentadiene in the gas mixture is inferred from the pressure of cyclopentadiene collected in the cylinder, leading to typical values ranging between 4.1 and 5.8%. Characterization of the final gas mixture is performed using a 25 cm^3 double-pass gas cell (Mettler Toledo) coupled to a FTIR spectrometer (Mettler Toledo, ReactIR ic 15). Figure 1 shows a typical FTIR spectrum of the cyclopentadiene−argon gas mixture.

The presence of impurities in the gas mixture is dispelled through inspection of the resulting IR spectra, specifically the absence of peaks around 2300−2400 cm^{-1} corresponding to the presence of CO_2 that would indicate a leak in the collection lines. Analysis of the vibrational assignments (see the Supporting Information) for the observed gas phase absorption bands are in good agreement with measurements by Gallinella et al.[58] The number density of cyclopentadiene in the reaction cell is inferred from the final molar fractions in the sample cylinder multiplied by the fraction of the cyclopentadiene/Ar mixture mass flow rate of the total mass flow rate. At 5.3 Torr and 298 K, the cell total number density is 1.7×10^{17} cm^{-3} with the cyclopentadiene number density ranging between $(0.2-1.2) \times 10^{14}$ cm^{-3} under typical experimental conditions.

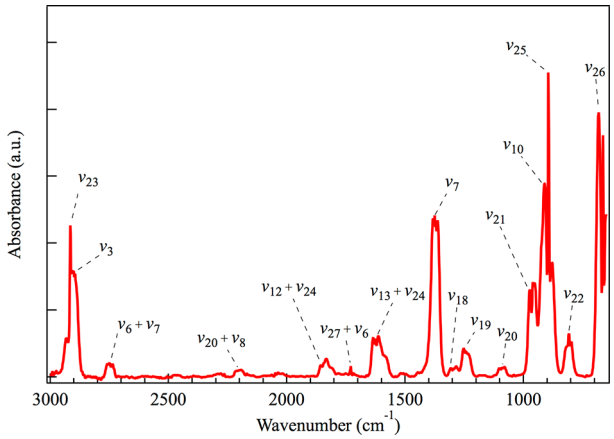

Figure 1. Baseline-subtracted infrared spectrum of the synthesized cyclopentadiene reactant in argon buffer gas. The vibrational bands are assigned according to analysis by Gallinella et al.[58]

2.2. Computational Methodology. The CH($X^2\Pi$) + $C_5H_6(X^1A_1)$ potential energy surface (PES) is calculated using the Gaussian 09 suite of programs.[59] Geometry optimizations and frequency calculations of all stationary points on the PES are first performed using hybrid DFT methods at the B3LYP/CBSB7 level.[60] Analysis of the resulting vibrational frequencies ensures that all stationary points are characterized as local minima or first-order saddle points. Single-point energy calculations are performed using the composite CBS-QB3 method to obtain more accurate energy values for all stationary points.[61−63] The transition states are located by scanning the bond lengths between intermediates using B3LYP/6-31G(d) and confirmed as first-order saddle points by the presence of an imaginary frequency. After single-point energy calculations on the transition state using the CBS-QB3 method, intrinsic reaction coordinate (IRC) calculations are then performed using B3LYP/6-31G(d) to verify the connectivity of the optimized transition state structures to the corresponding minima along the reaction coordinates. The described method was used to locate transition states for the entrance channels of the reaction; however, none were found.

3. EXPERIMENTAL RESULTS

3.1. Pseudo-First-Order Kinetics. The cyclopentadiene is introduced in excess relative to the CH radical. Under pseudo-first-order conditions, the CH LIF decay signal due to its reaction with cyclopentadiene is given by the following equations:

$$[CH]_t = [CH]_0 e^{-k_{1st}\Delta t} \quad (1)$$

$$k_{1st} = k_{2nd}[C_5H_6] + k'_{1st} \quad (2)$$

where k_{2nd} is the overall second-order rate constant of the CH(ν = 0) + cyclopentadiene reaction, Δt is the delay time between the photolysis and probe lasers, $[CH]_0$ and $[CH]_t$ refer to the CH radical concentrations initially in the cell and at a delay time (Δt), $[C_5H_6]$ is the number density of the cyclopentadiene introduced, k_{1st} is the pseudo-first-order rate constant for the CH radical decay, and k'_{1st} is the first-order rate

DOI: 10.1021/acs.jpca.9b03813
J. Phys. Chem. A 2019, 123, 5692−5703

constant for loss of CH by reaction with its precursor ($CHBr_3$) and other possible photoproducts such as CHBr, Br_2, Br, and CBr. For a constant bromoform flow rate, the concentrations of the precursor photolysis products remain constant within a given data set.

The integrated CH LIF signal is plotted against laser delay time for various cyclopentadiene number densities. The temporal profiles of the CH signal are fit using an exponential function in order to determine a value for k_{1st} using eq 1. Figure S4 displays temporal profiles of the LIF CH decay at 298 and 400 K for several number densities of cyclopentadiene. The k_{1st} values are then plotted against the cyclopentadiene number density to extract the overall second-order rate constant for the reaction as shown in eq 2. Figure 2

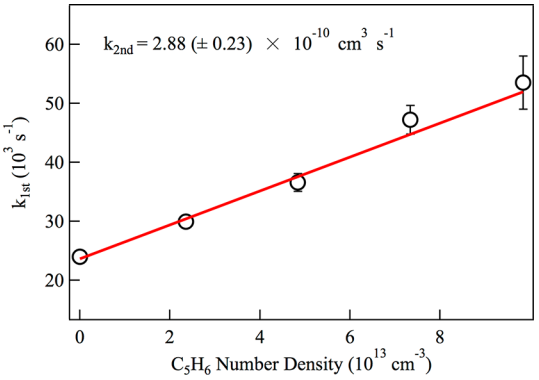

Figure 2. Typical plot of k_{1st} versus the number density of cyclopentadiene recorded at 298 K and 5.3 Torr. The k_{2nd} value is obtained using a linear fit to the data and reported with 2-standard deviation uncertainty.

shows a typical k_{2nd} plot recorded at 298 K and 5.3 Torr. The large pseudo-first-order rate measured in the absence of reactant is consistent with previously reported values under similar experimental conditions.[41,45,50,64] The fast CH decay is likely due to reaction with its precursor, molecular nitrogen, and any impurity in the buffer gas. The good linearity of the fit supports the pseudo-first-order approximation. The slope of the fit in Figure 2 is used to determine the second-order rate coefficient. The experimental procedure was preliminarily validated through determination of the second-order rate coefficient of the CH radical reaction with ethylene (C_2H_4). The weighted k_{2nd} value for the CH radical reaction with ethylene was measured to be $2.57(\pm0.14) \times 10^{-10}$ cm^3 s^{-1}, in good agreement with previous measurements.[45,49,65] Validation of the high temperature setup over the 298 to 450 K range has been achieved from previous experiments.[53,66] Table 1 displays the experimental conditions and measured rate coefficients for the CH + cyclopentadiene reaction.

The absorption cross section for cyclopentadiene has been measured to be 4.8×10^{-19} cm^2 at 266 nm,[67] and its dissociation at 248 nm is known to produce various reactive products, including the cyclopentadienyl (C_5H_5) and propargyl (C_3H_3) radicals. The photodissociation process may decrease the number density of reactants in the flow (within 5.5% to 7.0% of the initial reactant number density) and the photoproducts may react with the CH radical and interfere with the kinetic measurements. In order to investigate the effect of photolysis on the reaction rate coefficient, k_{2nd} values were measured as a function of laser fluence (total energy per unit surface). Figure S5 (Supporting Information) displays the measured rate coefficients as a function of laser fluence within the 88−112 mJ cm^{-2} range. The values for the laser fluence associated with the data set can be found in Table 1. The reaction rate coefficient displays no identifiable laser-fluence

Table 1. Experimental Conditions and Reported Overall CH + CPD Rate Coefficients for Independent Data Sets[a]

T (K)	η_{total} (10^{17} molecules cm^{-3})	[$CHBr_3$][b] (10^{13} molecules cm^{-3})	[CPD] range[c] (10^{12} molecules cm^{-3})	laser fluence (mJ cm^{-2})	k_{2nd} (10^{-10} cm^3 s^{-1})
298	1.74	2.11	27.8−116.1#	104	3.81 ± 0.25
298	1.72	2.23	23.6−98.6♦	111	2.97 ± 0.15
298	1.74	2.28	23.9−99.9♦	110	2.82 ± 0.36
298	1.74	2.14	23.9−99.9♦	111	2.31 ± 0.20
298	1.72	2.25	23.5−98.4♦	108	2.46 ± 0.20
298	1.72	2.21	23.9−99.8*	111	2.52 ± 0.18
298	1.72	2.17	24.1−100.7	110	3.69 ± 0.27
298	1.73	2.17	23.6−98.5°	92	2.88 ± 0.23
298	1.72	2.37	27.3−114.2•	92	3.37 ± 0.14
298	1.71	2.16	27.1−113.4•	88	3.61 ± 0.18
298	1.74	2.35	24.1−100.9*	99	2.43 ± 0.24
298	1.74	2.36	24.1−100.9*	94	1.68 ± 0.15
298	3.13	3.80	50.3-210.3#	104	2.85 ± 0.32
298	0.90	1.25	12.5−52.1*	108	3.17 ± 0.38
350	1.49	2.30	20.3−84.7°	92	3.42 ± 0.26
350	1.51	2.21	20.5−85.8°	92	2.83 ± 0.30
350	1.55	2.50	24.6−102.7•	88	2.54 ± 0.27
400	1.32	2.15	18.0−75.2°	92	1.99 ± 0.21
400	1.35	2.29	18.3−76.6°	92	3.10 ± 0.21
400	1.41	2.55	17.6−74.4•	88	2.57 ± 0.15
450	1.29	2.80	20.6−86.0•	92	1.98 ± 0.89
450	1.31	2.69	16.5−69.3•	88	2.19 ± 0.14

[a]Reported error is 2σ obtained from the linear fit of the k_{2nd} plots. [b][$CHBr_3$] fluctuations are within 5% of the reported average. [c]The marks indicate data sets recorded with the same CPD mixture cylinder.

DOI: 10.1021/acs.jpca.9b03813
J. Phys. Chem. A 2019, 123, 5692−5703

dependence within the investigated fluence range. Any dependence on the laser fluence is within two standard deviation of the overall rate coefficient; however, the effect of CPD photoproducts and their subsequent side reactions on the measure rate coefficients cannot be entirely dismissed. These reactions, in conjunction with differences in the precursor concentrations listed in Table 1, are likely to contribute to the overall large spread of the k_{2nd} values. In Table 1, the marks indicate data sets recorded with the same CPD mixture cylinder. The large spread in the measured k_{2nd} is unlikely to be due to uncertainties on the reactant concentrations but more likely to the effect of CPD photolysis.

3.2. Pressure and Temperature Dependence. The pressure dependence of the overall CH + cyclopentadiene rate coefficient is studied over the 2.7−9.7 Torr range. Figure 3

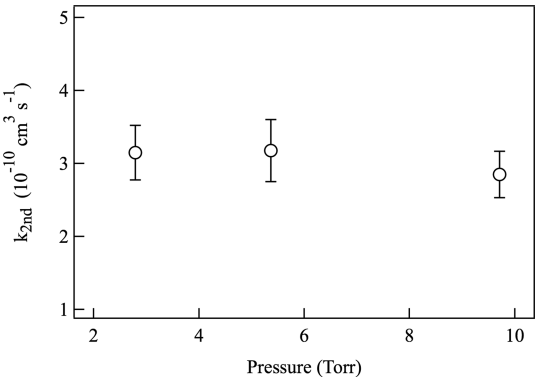

Figure 3. Second-order rate coefficient (k_{2nd}) as a function of total cell pressure at 298 K. Each data point is from the average of multiple runs with error bars reported to 2σ precision.

shows the second-order rate coefficients reported with vertical error bars representing 2σ error over the specified pressure range. The standard deviation is obtained by weighting the k_{1st} values by the 2σ error obtained from the individual linear fits versus cyclopentadiene number density plots. The k_{2nd} values for each corresponding point are averaged from at least three independent data sets obtained from different cyclopentadiene samples. The individual rate constants over the specified range of pressure are in good agreement within 2σ error of each other. This suggests that the second-order rate constant is pressure independent over the specified experimental range.

The temperature dependence of the overall rate constant of the CH + cyclopentadiene reaction is studied over the 298−450 K range. Figure 4 shows the second-order rate constants over the full experimental range and a pressure range of 5.3−6.1 Torr. The data up to 400 K are reported as the weighted average of the independent data sets with vertical error bars representing 2σ error. The weighted average k_{2nd} values shown in Figure 4 are reported as $2.70(\pm1.34) \times 10^{-10}$ cm^3 molecule^{-1} s^{-1} for 298 K, $2.94(\pm0.90) \times 10^{-10}$ cm^3 molecule^{-1} s^{-1} for 350 K, and $2.56(\pm1.19) \times 10^{-10}$ cm^3 molecule^{-1} s^{-1} for 400 K. At 450 K only two independent data sets were obtained due to difficulties arising from optimization of the CH LIF signal at higher temperatures. For the 450 K data, the unweighted average is recorded, and the uncertainty reported as the minimum and maximum values of the two data sets. The individual rate constants over the specified range of temperature are in good agreement within 2σ error of each other,

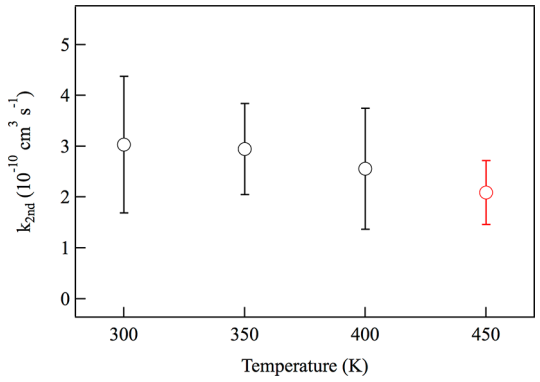

Figure 4. Second-order rate coefficient as a function of the cell temperature over the 5.3−6.1 Torr cell pressure range. Each data point is a weighted average from at least three independent data sets with error bars reported to 2σ precision. The 450 K point (red circle) is the average of two data sets reported with the minimum and maximum values.

suggesting no observable temperature dependence over the specified experimental temperature range.

4. CH($X^2\Pi$) + CYCLOPENTADIENE POTENTIAL ENERGY SURFACE

Part of the C_6H_7 potential energy surface has been computed for the CH cycloaddition and insertion mechanisms using DFT and CBS-QB3 calculations to complement the kinetic results. All of the energy values provided are relative to the reactants: cyclopentadiene and the CH radical. Figure 5 shows

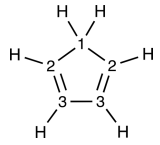

Figure 5. Representation of the CH radical reaction sites of cyclopentadiene for the purposes of discussion of the potential energy surface entrance channels.

the C_{2v} symmetry in the structure where the sp^3 hybridized carbon is labeled C1 and the remaining sp^2 carbons are described as C2 and C3, respectively. The PES is split into two separate pathways by way of the entrance channel mechanism. The enthalpies for the products of the hydrogen abstraction pathways as well as several acyclic products are computed and examined further in the Discussion section but are not included in the displayed PES.

A comparison of the energetics from previous C_6H_7 PES theoretical calculations to the present calculations can be found in the Supporting Information. Calculated values for the PES are in good agreement with the previous studies; any discrepancies in the values are due to the differences in the method and level of theory used for the calculation. It is worth noting that some H-elimination transition states leading to the formation of fulvene were not located in this study but were identified using higher-level methods by Melius et al.[68] and Jasper et al.[52] These barriers are within the error of the CBS-QB3 method and should be considered negligible as they are significantly small and all of the computed product channels are highly exothermic relative to the reactants.

DOI: 10.1021/acs.jpca.9b03813
J. Phys. Chem. A 2019, 123, 5692−5703

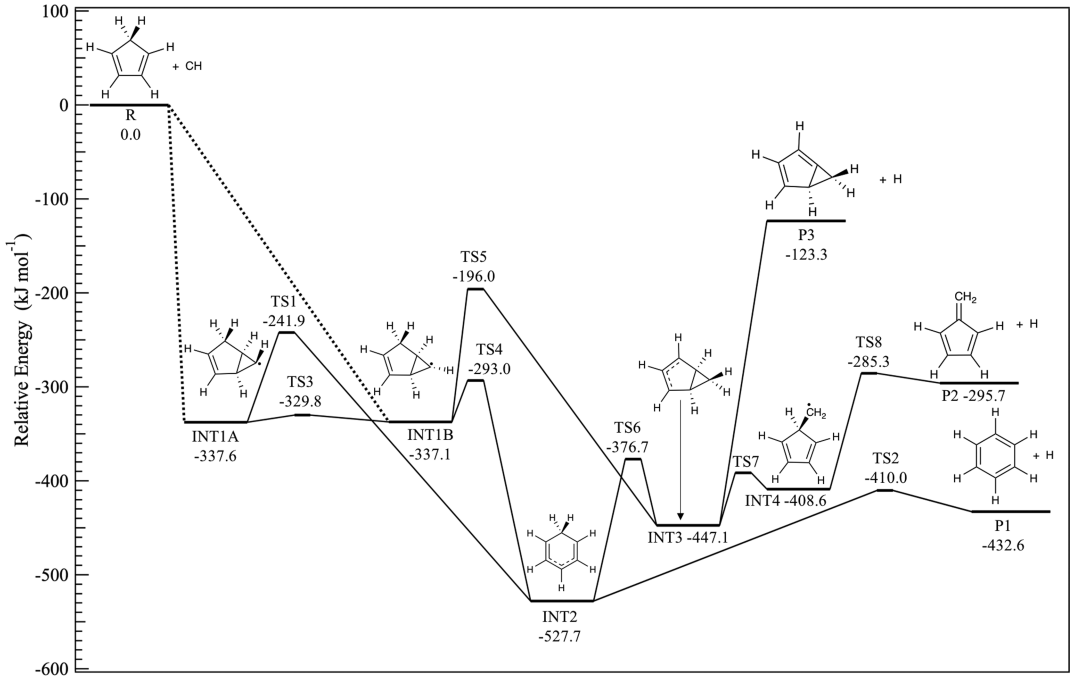

Figure 6. Schematic of the C_6H_7 potential energy surface proceeding through CH cycloaddition onto the C═C bond of the cyclopentadiene reactant.

4.1. CH Cycloaddition Mechanism. Figure 6 displays part of the potential energy surface for the CH radical cycloaddition across C2 and C3 of cyclopentadiene. The CH cycloaddition mechanism consists of two entrance channels and three exit channels through H-loss to form benzene (P1), fulvene (P2), and bicyclo[3.1.0]hexa-1,3-diene (P3). Two exothermic bicyclic intermediates are formed from the CH cycloaddition entrance channel: INT1A, for which the CH substituent is oriented toward the ring structure, and INT1B, where the CH substituent is oriented away from the ring structure. The slight structural difference between the two intermediates leads to an 0.5 kJ mol^{-1} energy difference. Isomerization from INT1A to INT1B can occur through a barrier of 7.3 kJ mol^{-1} relative to INT1B. INT1A can also undergo a ring opening through TS1 with relative energetics of 95.7 kJ mol^{-1} to form the resonance stabilized six-membered ring intermediate INT2. The formation of INT2 is exothermic by 527.7 kJ mol^{-1} relatively to the reactants. Formation of INT2 is the most thermodynamically exothermic channel identified on the PES due to resonance stabilization of the radical along the π-electron system of the structure. INT2 can subsequently eliminate a hydrogen from carbon C1 through TS2 lying 117.7 kJ mol^{-1} above INT2 to form benzene. The formation of benzene and a hydrogen atom is the most thermodynamically accessible pathways with a reported energy of −432.6 kJ mol^{-1} relative to the reactants. INT1B can also ring open to form the stable six-membered ring INT2 through TS4 lying at 44.1 kJ mol^{-1} above INT1B and follow the same previously mentioned hydrogen elimination pathway to form benzene. The transition state to INT2 from INT1B is 51.1 kJ mol^{-1} less than for the corresponding pathway from INT1A due to the differences in the orientation of the CH substituent.

INT1B can also undergo a 1,3-hydrogen shift from the neighboring C1 through TS5 lying 141.1 kJ mol^{-1} above INT1B to form the bicyclic intermediate INT3, which has thermodynamically accessible pathways to all three of the major products on the PES. INT3 decomposes through H-loss from C2 through a barrierless dissociation channel to form the bicyclic product P3. The products, P3 and a hydrogen atom, have the highest energetics of the three products at −123.3 kJ mol^{-1} relative to the reactants. INT3 can also ring expand through breaking of the bond between C2 and C3 of the five-membered ring to form the six-membered ring INT2 through TS6, lying 70.4 kJ mol^{-1} above INT3. This can ultimately lead to the formation of benzene through TS2 as previously described. The methylene-substituted cyclopentadiene INT4 can form from breaking of the bond between the bicyclic substituent and C2 of the larger ring on INT3. TS7 is 55.9 kJ mol^{-1} above INT3, and INT4 has a relative energy of 408.6 kJ mol^{-1} below the reactants. INT4 can further lose the remaining hydrogen substituent on C1 through TS8 that lies 123.3 kJ mol^{-1} above it to form P2, fulvene. The fulvene and a hydrogen atom product set, has a relative energy of 295.7 kJ mol^{-1} below that of the reactants.

4.2. CH Insertion Mechanism. Figure 7 shows the PES for the barrierless insertion pathways along the three possible entrance channels to form three initial methylene-substituted intermediates: INT4, INT5, and INT7. Due to the C_{2v} symmetry of cyclopentadiene, there are three sites for the CH radical to insert into the C—H bonds of the molecule: the sp^3 carbon atom (C1) or either of the two sp^2 carbon atoms along the C═C bond (C2 or C3). Insertion of the CH radical into the C—H bond of C2 leads to INT7 with a reported energy of 509.7 kJ mol^{-1} below the reactants. Similarly, the CH radical can insert into the C−H bond of C3 to form INT5 that is 485.9 kJ mol^{-1} below the reactants. Both INT5 and INT7 can isomerize to each other through TS11, which is 121.1 kJ mol^{-1} above INT5. INT5, INT6, and INT7 can individually undergo hydrogen elimination from respective sp^3 carbons to form fulvene, likely proceeding through small energy barriers as calculated previously elsewhere.[51,52] Insertion of the CH radical into C1 produces INT4, which also results from the

DOI: 10.1021/acs.jpca.9b03813
J. Phys. Chem. A 2019, 123, 5692−5703

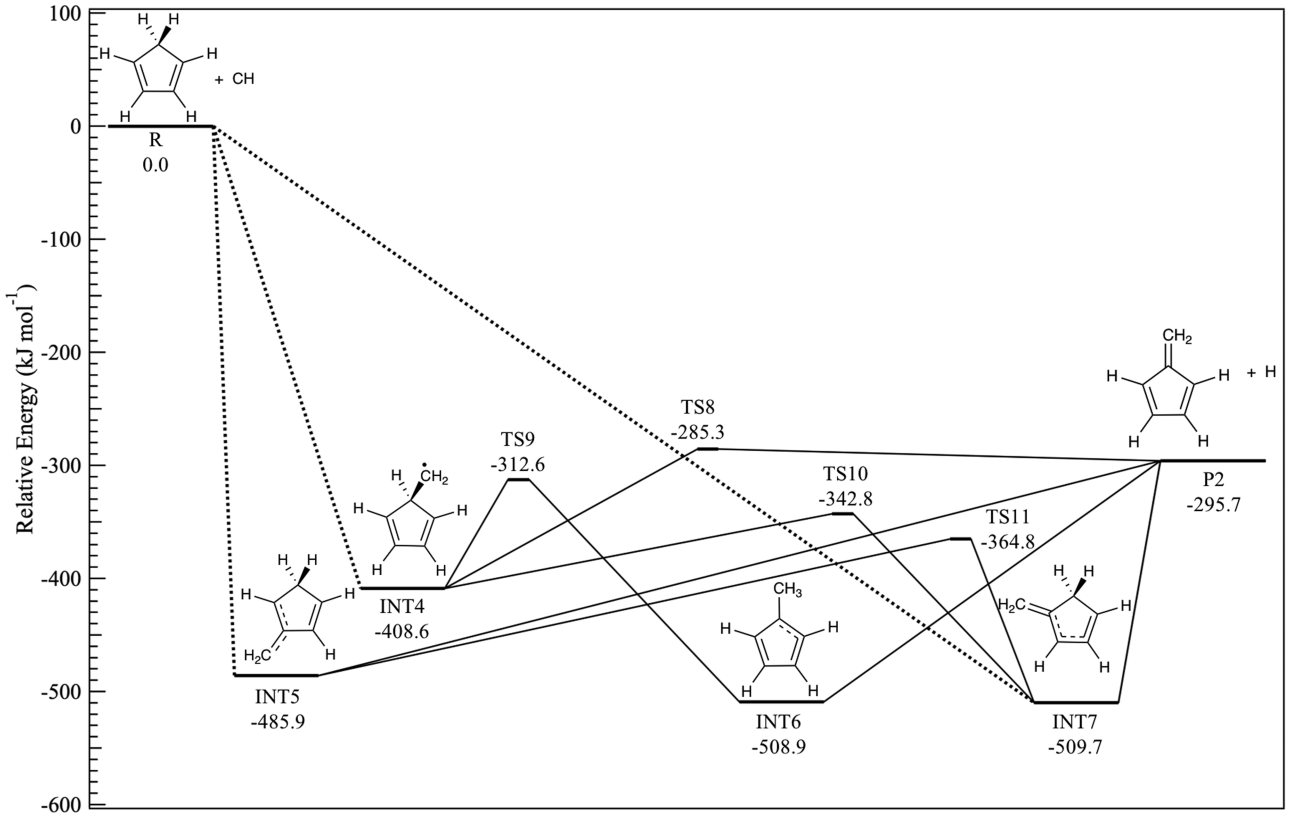

Figure 7. Schematic of the C_6H_7 potential energy surface proceeding through CH insertion into the C−H bonds of the cyclopentadiene reactant.

ring opening of INT3 along the cycloaddition pathway as discussed in the previous section (see Figure 6).

INT4 is the connecting intermediate between the CH cycloaddition and CH insertion mechanisms and can follow three pathways to form fulvene: two of which involve hydrogen migration and the third involves the previously described hydrogen elimination from C1 through TS8. A 1,2-hydrogen migration can occur on INT4 to isomerize to the methylcyclopentadienyl intermediate, INT6, through TS9, which lies 96.0 kJ mol^{-1} above INT4. From INT6, barrierless hydrogen-loss from the methyl group of the intermediate leads to the formation of fulvene. A 1,3-hydrogen migration can also occur on INT4 through a barrier of 65.8 kJ mol^{-1} to form the C2 methylene-substituted INT7.

5. DISCUSSION

The kinetics of the CH ($X^2\Pi$) + cyclopentadiene reaction were determined experimentally between 298 and 450 K and at 2.7−9.7 Torr. The lack of pressure dependence and the average rate coefficient of $2.70(\pm1.34) \times 10^{-10}$ cm^3 molecule^{-1} s^{-1} for 298 K, as shown in Figure 3, are in agreement with the rapid, pressure independent rate coefficients found in previous studies of CH radical reactions with unsaturated hydrocarbons. The pressure independence of the measured rate coefficients together with the good exponential fits of the CH decays suggest that the reaction is already performed at or near the high-pressure limit with negligible dissociation of the initial reaction adduct. The temperature independence of the rate constants over the experimental range in Figure 4 is in agreement with the absence of an energy barriers, which is consistent with the widely accepted mechanism of CH radical reactions with unsaturated hydrocarbons, as first proposed by Berman et al.[45] The experimental rate coefficients reported here are fast and already near the collision limit and thus increasing the number of π-bonds in the reactant molecule is not expected to dramatically affect the overall rate coefficient. Reported experimental rate coefficients ($(2.81-4.18) \times 10^{-10}$ cm^{-3} s^{-1} between 235 and 470 K) for the reaction of CH + anthracene ($C_{15}H_{10}$)[50] do not drastically differ from the CH + cyclopentadiene values despite π-bond conjugation among the three-ringed reactant. Similarly, room temperature rate coefficients from C(^{3}P) reactions with C_2H_2, C_2H_4, and C_6H_6, reported at 2.4×10^{-10}, 2.1×10^{-10}, and 2.8×10^{-10} cm^3 s^{-1}, respectively, reveal no increase in the rate coefficient despite an increase in the π-bonding sites.[69]

The non-Arrhenius temperature dependence of the fast rate coefficient is likely to be due to a strongly attractive potential driven by long-range electrostatic forces between the reactants (i.e., adiabatic capture) in agreement with Canosa et al.[40] and as discussed in the reviews by Stoecklin et al.[70] and Clary.[71] The lack of a potential energy barrier on the PES further supports a strong interaction potential between the reactants, as suggested by Clary.[71] This strong attractive potential would likely encourage CH insertion cycloaddition onto the π-bonds of CPD over CH as the preferred entrance mechanism at ambient temperatures. It is difficult to comment on the temperature dependence for this reaction outside of the temperature range examined here. As discussed in the Introduction, similar CH radical reactions have shown a change in temperature dependence at low temperatures when the reaction is governed by long-range potential between the reactants. Although further experiments and Master Equation studies are necessary to expand upon the temperature range, it is unlikely that the reaction rate for the addition of the CH

DOI: 10.1021/acs.jpca.9b03813
J. Phys. Chem. A 2019, 123, 5692−5703

onto the CPD unsaturation changes considerably above 450 K. Any change in the observed reaction rate coefficient for the title reaction is more likely to be due to the abstraction mechanisms becoming more favorable, as discussed further in this section.

The experimentally determined rate coefficients support a barrierless entrance channel that proceeds either through CH cycloaddition across the C═C bond or CH insertion into a C—H bond of the five-membered ring. Although transition states for these entrance channels could not be located with the level of theory employed here, previous computational and experimental studies of CH radical reactions with unsaturated hydrocarbons have shown that the CH cycloaddition and insertion are in general barrierless processes.[36,72−74] Ribeiro et al.[48] calculated the minimal energy profiles for the transition states of the entrance channels for the CH + propane reaction using B3LYP/6-311G(d,p) level of theory. They concluded that all three entrance channels were in fact barrierless, showing a decrease in energy as the bond length of interest decreased. They later reported similar results for the entrance channels of CH + propene reaction.[72] In this case they performed calculations of various reactive trajectories between the molecules to determine the probability of either CH insertion or CH addition occurring. From these calculations they were able to conclude that CH cycloaddition across the C═C bond is likely to dominate with branching ratios of 85:15, which is in good agreement with experimental product detection studies for this reaction.[47] Based upon previous studies[36,72−74] and the experimental evidence from the kinetics provided here, it is reasonable to assume that the entrance channels for this reaction are indeed barrierless.

Since no experimental information about the products can be inferred from the kinetic data presented here, a PES is proposed on the basis of similar CH radical reaction mechanisms. In this paragraph the discussion of the reaction products is purely based on enthalpic considerations and are intended only for supporting the kinetic measurements. These results will be complemented in an upcoming publication by statistical calculations including entropic factors. The energetics for the intermediates and transitions states in Figures 6 and 7 are in good agreement with earlier C_6H_7 PES involving the formation of benzene and/or fulvene.[12,51,52,68,75−78] As described in Figure 6, the initial intermediates INT1A and INT1B are formed through fast, barrierless cycloaddition and can immediately ring-open to INT2, from which H-elimination can occur to give C_6H_6 products. The resonantly stabilized INT2 is highly exothermic relative to the reactants and products. Under the present experimental conditions, it is unlikely that any intermediates are stabilized in the reaction cell. Adducts formed from CH addition to unsaturated hydrocarbon systems have very short lifetimes and have a propensity to isomerize and dissociate with rates much greater than the collisional quenching rate with the buffer gas.[79] Once formed, INT2 is therefore likely to isomerize or directly dissociate. As shown by Dubnikova and Lifshitz[76] in their theoretical investigation of ring expansion mechanisms of methylcyclopentadiene radicals, the increase in the bond length of the CH_2 site in INT2 indicates a weakening of the C—H and a greatly facilitated H-loss channel. Dissociation is therefore likely to dominate over isomerization back to either of the initial intermediates or INT3. These ring contraction channels are expected be entropically less favorable than dissociation.

The portion of the PES for the CH insertion entrance channel shown in Figure 7 only includes the product channels for fulvene + H, despite accessible pathways to the other two products. INT4, where CH insertion occurs on the sp^3 hybridized carbon, serves as the connecting intermediate between the two PES and is also capable of ring-expansion. Direct ring-expansion routes to the formation of benzene + H from INT5 and INT7, where CH insertion occurs on either of the sp^2 hybridized carbons, are also possible and have been calculated by Dubnikova and Lifshitz.[76] Both pathways involve an additional intermediate and transition state compared to the ring-opening pathway from INT4 to INT2 in Figure 6. However, the authors conclude that the benzene formation pathways from INT5 and INT7 have much higher barriers than that for isomerization to INT4 and subsequent rate constant calculations favor the isomerization of INT5 and INT7 to INT4 versus direct ring-expansion pathways. A favored isomerization of INT 5 and INT7 into INT4 opens up pathways to the formation of the bicyclic product P3. For these reasons, the product channels for benzene and P3 remain competitive regardless of the dominant entrance channel. Although formation of benzene is the thermodynamically minimum energy pathway, an appreciable amount of fulvene and bicyclic product can also be expected to form considering that all of the product channels are well below the energy of the reactants and thermodynamically accessible. RRKM and Master Equations calculations are required to fully conclude on the probability of benzene formation and will be the subject of future publications.

In order to discuss the possibility of H-abstraction pathways, the enthalpies of reaction for the CH_2 coproducts were calculated. Table 2 displays the computed enthalpies of reaction for the H-abstraction products together with H-elimination products for comparison. The abstraction of a H atom from the three sites on the cyclopentadiene molecule leads to the formation of three isomers of cyclopentadienyl. Two of these channels, abstraction from the C2 and C3 sites, are thermodynamically unfavorable relative to the reactants. Abstraction from the C1 site results in the formation of a cyclopentadienyl moiety and a CH_2 carbene, 39.3 kJ mol^{-1} below the reactants. H-abstraction from the C2 or C3 site also results in a cyclopentadienyl moiety but with respective relative energetics of 99.5 and 97.2 kJ mol^{-1} above the reactants. The disparity in these relative enthalpies compared to those for the C1 abstraction can be attributed to the hybridization of the site and difference in the C—H bond lengths. Additionally, abstraction from the C1 site results in electron delocalization

Table 2. Enthalpies of Reaction for the H-Elimination and Abstraction Pathways for the CH + Cyclopentadiene Reaction

H-Elimination Products	$\Delta_r H$ (298K) (kJ · mol^{-1})	H-Abstraction Products	$\Delta_r H$ (298K) (kJ · mol^{-1})
Bicyclo[3.1.0]hexa-1,3-diene + H	-123.3	c-C_5H_5 + CH_2	-39.3
Fulvene + H	-295.7	2-C_5H_5 + CH_2	+99.5
Benzene + H	-432.6	3-C_5H_5 + CH_2	+97.2

DOI: 10.1021/acs.jpca.9b03813
J. Phys. Chem. A 2019, 123, 5692−5703

on the five-membered ring that lends to the overall stability of the molecule. The calculated C—H bond lengths on the sp^3 hybridized C1 site were approximately 1.099 Å, compared to 1.082 Å reported for the C—H bonds on the sp^2 hybridized C2 and C3 sites, indicating a longer bond that helps to facilitate the H-abstraction on the C1 site. In general, for CH radical reactions, H-abstraction pathways are unfavorable due to higher barriers and have not be observed experimentally for other CH radical reactions with small linear hydrocarbons.[42,48,72,80] In the case of the CH radical reaction with propane, Ribeiro et al.[48] searched for the transition states for H-abstraction pathways but could not locate saddle points on the corresponding PES. Any attempt to locate the transition state led toward the energetically favorable CH insertion channel, leading the authors to conclude that CH is more likely to insert into a C—C or C—H bond rather than abstract a hydrogen despite the fact that the H-abstraction products were energetically accessible. A similar fate was found for the CH radical approach to the propene molecule in another study by the same authors.[72] The CH cycloaddition and insertion pathways are considered much more energetically favorable and thus more competitive pathways than the H-abstraction pathway, which is not included in the C_6H_7 PES for these reasons.

Pathways to formation of acyclic C_6H_6 products are not explored in depth for purposes of the C_6H_7 PES presented here. Several of the linear products were calculated using the aforementioned DFT and CBS-QB3 methods and found to be thermodynamically accessible. The acyclic products considered are typical of C_6H_6 formation reactions (e.g., propargyl radical self-recombination[81,82]) and are shown in Table 3. The formation of linear products would involve the inclusion of extra ring-opening and hydrogen migration steps that are not consistent with previously accepted CH radical mechanisms. Additional ring-openings would likely involve scissions of INT2, after the initial ring-opening step from the bicyclic intermediates, or any of the CH insertion intermediates (INT4, INT5, and INT7). The additional intermediates and transition states from this ring-opening could still be thermodynamically accessible, as the pathways described are already highly exothermic relative to the reactants. It is arguable that these additional pathways would likely involve higher barriers relative to the ones discussed here due to loss of resonance-stabilization in the intermediate ring structures, making the formation of acyclic products less favorable in comparison to their ringed counterparts.

Table 3. Relative Enthalpies of Formation for Several of the Acyclic Isomers of C_6H_6: 1,2-Hexadiene-5-yne (1,2-HD5Y); 1,5-Hexadiyne (1,2-HD5Y); 2-Ethynyl-1,3- butadiene (2*E*-1,3-BD); 1,3-Hexadiene-5-yne (1,3-HD5Y); 1,2,4,5-Hexatetraene (1,2,4,5-HT)

Acyclic C_6H_6 Isomers		$\Delta_f H$ (298K) (kJ · mol^{-1})
1,2-HD5Y + H	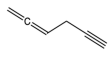 + H	-91.5
1,5-HDY + H	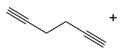 + H	-89.9
2E-1,3-BD + H	 + H	-161.2
1,3-HD5Y + H	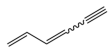 + H	-151.8
1,2,4,5-HT + H	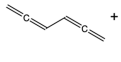 + H	-113.0

6. CONCLUSION AND IMPLICATIONS FOR COMBUSTION CHEMISTRY

The experimental reaction rate for the CH radical reaction with cyclopentadiene is fast, near the collision limit, and could potentially reveal a pathway to the formation of the "building block" aromatic benzene in the combustion fuels. The presence of both the CH radicals and cyclopentadiene molecule in these various combustion systems lends particular significance to the potential for inclusion in models. The need for the expansion of sophisticated models continues to grow, especially as energy dependences shift outside fossil fuel sources. In biomass combustion, the fragmentation of lignin monomers produces significant amounts of cyclopentadiene, where subsequent reactions are believed to be competitive routes alongside the HACA mechanism to PAH formation.[83] Composition studies of the exhaust emissions from the combustion of attractive biofuel candidate, dimethylfuran, reveal first-ring intermediates, cyclopentadiene and benzene, as key products.[84] Likewise, the combustion of many synthetically produced high-energy-density hydrocarbon fuels (HEDHFs), appealing for their efficiency in energy output and decrease in required volume, yield similar products. The thermal decomposition investigations of one such synthetic fuel, tetrahydrotricyclopentadiene ($C_{10}H_{16}$), generates cyclopentadiene and benzene as major products.[85,86] Despite the advancements in studying alternative fuel sources, the roles of first hydrocarbon rings like cyclopentadiene and benzene remains persistent.

Ring-expansion mechanisms, in particular from five to six-membered rings, could offer valuable insight into the rate limiting step of these gas phase molecular growth schemes. Portions of the C_6H_7 potential energy surface presented here overlap with other combustion-relevant ring-expansion reactions like CH_3 radical reactions with cyclopentadienyl[12,78,87,88] as well as the H-assisted isomerization of fulvene to benzene,[51,52] where computational models support the formation of benzene as the major product at higher temperatures (>1000 K). The fast, pressure-independent rate coefficients support the formation of C_6H_6 isomers, proceeding through thermodynamically accessible pathways. The formation of benzene and a hydrogen is the most thermodynamically favored product with reported energetics relative to the reactants of 432.6 kJ mol^{-1}. In addition, the formation of fulvene and a hydrogen is expected to be non-negligible and can further react through H-assisted isomerization or other molecular growth schemes. At higher temperatures other pathways may become more favorable, such as the H abstraction to produce cyclopentadienyl, which is a key reactive intermediate in PAH formation mechanisms of combustion reactions.

The abundance of these reactant species in high-pressure, high-temperature systems supports a need for inclusion of the reaction rate into combustion models. CH radicals are highly

DOI: 10.1021/acs.jpca.9b03813
J. Phys. Chem. A 2019, 123, 5692−5703

reactive and their reactions with unsaturated hydrocarbons allow for ring expansion in molecules. The fast pressure-independent rate coefficients from the CH + cyclopentadiene reaction presented here advocate the formation of C_6H_6 isomers that play a crucial role in combustion. The lack of temperature dependence in the rate coefficients further suggests that CH cycloaddition, driven by a strong attractive potential between the reactants, is likely to dominate over insertion or abstraction mechanisms at room temperature. Fulvene and benzene are likely to form as major products for this reaction, supported by thermodynamically accessible pathways. At combustion relevant temperatures (>800 K), H-abstraction pathways could become more significant, becoming a larger source of cyclopentadienyl radicals. Further kinetic studies at higher temperatures are necessary to confirm these mechanisms. Ongoing experiments and theoretical studies are being performed in order to further confirm and quantify the identities of the products for the title reaction.

■ ASSOCIATED CONTENT

Supporting Information

The Supporting Information is available free of charge on the ACS Publications website at DOI: 10.1021/acs.jpca.9b03813.

Details of cyclopentadiene synthesis, cyclopentadiene characterization through NMR and gas-phase FTIR, vibrational assignments of gas phase cyclopentadiene, temporal LIF CH decay profiles, laser fluence dependence, comparison of C_6H_7 PES calculations, and vibrational frequencies, rotational constants, and CBS-QB3 energies for all stationary points (PDF)

■ AUTHOR INFORMATION

Corresponding Author

*Email: Fabien.Goulay@mail.wvu.edu.

ORCID

F. Goulay: 0000-0002-7807-1023

Notes

The authors declare no competing financial interest.

■ ACKNOWLEDGMENTS

The authors acknowledge the financial support from the WVU Research Corporation through the Program to Stimulate Competitive Research. The authors also thank the West Virginia University High Performance Computing shared facility for providing computing resources and Dr. Novruz G. Akhmedov for the NMR analysis of the cyclopentadiene reactant. F.G., K.L.C., and Z.N.D. are grateful to the National Science Foundation for its support of this work through Grant CHE-1764178. Z.N.D. acknowledges support from the Summer Undergraduate Research Experience (SURE) program at WVU. T.M.S. thanks the Washington County Campus Foundation for financial support for this research.

■ REFERENCES

(1) Richter, H.; Howard, J. B. Formation of Polycyclic Aromatic Hydrocarbons and Their Growth to Soot: A Review of Chemical Reaction Pathways. *Prog. Energy Combust. Sci.* **2000**, *26*, 565−608.

(2) Frenklach, M. Reaction Mechanism of Soot Formation in Flames. *Phys. Chem. Chem. Phys.* **2002**, *4*, 2028−2037.

(3) Krasnopolsky, V. A. A Photochemical Model of Titan's Atmosphere and Ionosphere. *Icarus* **2009**, *201* (1), 226−256.

(4) Cherchneff, I.; Barker, J. Polycyclic Aromatic Hydrocarbons and Molecular Equilibria in Carbon-Rich Stars. *Astrophys. J.* **1992**, *394*, 703−716.

(5) Brownsword, R. A.; Sims, I. R.; Smith, I. W. M.; Stewart, D. W. A.; Canosa, A.; Rowe, B. R. The Radiative Association of CH with H_2: A Mechanism for Formation of CH_3 in Interstellar Clouds. *Astrophys. J.* **1997**, *485*, 195−202.

(6) Puget, J. L.; Léger, A. A New Component of the Interstellar Matter: Small Grains and Large Aromatic Molecules. *Annu. Rev. Astron. Astrophys.* **1989**, *27* (1), 161−198.

(7) Frenklach, M.; Feigelson, E. Formation of Polycyclic Aromatic Hydrocarbons in Circumstellar Envelopes. *Astrophys. J.* **1989**, *341*, 372−384.

(8) Johansson, K. O.; Head-Gordon, M. P.; Schrader, P. E.; Wilson, K. R.; Michelsen, H. A. Resonance-Stabilized Hydrocarbon-Radical Chain Reactions May Explain Soot Inception and Growth. *Science* **2018**, *361* (6406), 997−1000.

(9) Parker, D. S. N.; Kaiser, R. I.; Troy, T. P.; Ahmed, M. Hydrogen Abstraction/Acetylene Addition Revealed. *Angew. Chem., Int. Ed.* **2014**, *53* (30), 7740−7744.

(10) Yang, T.; Kaiser, R. I.; Troy, T. P.; Xu, B.; Kostko, O.; Ahmed, M.; Mebel, A. M.; Zagidullin, M. V.; Azyazov, V. N. HACA's Heritage: A Free-Radical Pathway to Phenanthrene in Circumstellar Envelopes of Asymptotic Giant Branch Stars. *Angew. Chem., Int. Ed.* **2017**, *56* (16), 4515−4519.

(11) D'Anna, A.; Violi, A. A Kinetic Model for the Formation of Aromatic Hydrocarbons in Premixed Laminar Flames. *Symp. Combust., [Proc.]* **1998**, *27* (1), 425−433.

(12) Melius, C. F.; Colvin, M. E.; Marinov, N. M.; Pit, W. J.; Senkan, S. M. Reaction Mechanisms in Aromatic Hydrocarbon Formation Involving the C_5H_5 Cyclopentadienyl Moiety. *Symp. Combust., [Proc.]* **1996**, *26*, 685−692.

(13) Mulholland, J. A.; Lu, M.; Kim, D.-H. Pyrolytic Growth of Polycyclic Aromatic Hydrocarbons by Cyclopentadienyl Moieties. *Proc. Combust. Inst.* **2000**, *28* (2), 2593−2599.

(14) Pope, C. J.; Miller, J. A. Exploring Old and New Benzene Formation Pathways in Low-Pressure Premixed Flames of Aliphatic Fuels. *Proc. Combust. Inst.* **2000**, *28*, 1519.

(15) Castaldi, M. J.; Marinov, N. M.; Melius, C. F.; Huang, J.; Senkan, S. M.; Pitz, W. J.; Westbrook, C. K. Experimental and Modeling Investigation of Aromatic and Polycyclic Aromatic Hydrocarbon Formation in a Premixed Ethylene Flame. *Symp. Combust., [Proc.]* **1996**, *26*, 693−702.

(16) Ruwe, L.; Moshammer, K.; Hansen, N.; Kohse-Höinghaus, K. Influences of the Molecular Fuel Structure on Combustion Reactions towards Soot Precursors in Selected Alkane and Alkene Flames. *Phys. Chem. Chem. Phys.* **2018**, *20* (16), 10780−10795.

(17) Hansen, N.; Miller, J. A.; Klippenstein, S. J.; Westmoreland, P. R.; Kohse-Höinghaus, K. Exploring Formation Pathways of Aromatic Compounds in Laboratory-Based Model Flames of Aliphatic Fuels. *Combust., Explos. Shock Waves* **2012**, *48* (5), 508−515.

(18) Wang, H. A.; Frenklach, M. A Detailed Kinetic Modeling Study of Aromatics Formation in Laminar Premixed Acetylene and Ethylene Flames. *Combust. Flame* **1997**, *2180* (97), 173−221.

(19) Vandewiele, N. M.; Magoon, G. R.; Van Geem, K. M.; Reyniers, M. F.; Green, W. H.; Marin, G. B. Experimental and Modeling Study on the Thermal Decomposition of Jet Propellant-10. *Energy Fuels* **2014**, *28* (8), 4976−4985.

(20) Knyazev, V. D.; Popov, K. V. Kinetics of the Self Reaction of Cyclopentadienyl Radicals. *J. Phys. Chem. A* **2015**, *119* (28), 7418−7429.

(21) Kim, D. H.; Mulholland, J. A.; Wang, D.; Violi, A. Pyrolytic Hydrocarbon Growth from Cyclopentadiene. *J. Phys. Chem. A* **2010**, *114* (47), 12411−12416.

(22) Savee, J. D.; Selby, T. M.; Welz, O.; Taatjes, C. A.; Osborn, D. L. Time- and Isomer-Resolved Measurements of Sequential Addition of Acetylene to the Propargyl Radical. *J. Phys. Chem. Lett.* **2015**, *6* (20), 4153−4158.

DOI: 10.1021/acs.jpca.9b03813
J. Phys. Chem. A 2019, 123, 5692−5703

(23) Wang, H.; Brezinsky, K. Computational Study on the Thermochemistry of Cyclopentadiene Derivatives and Kinetics of Cyclopentadienone Thermal Decomposition. *J. Phys. Chem. A* **1998**, *102* (9), 1530−1541.
(24) Brezinsky, K. The High-Temperature Oxidation of Aromatic Hydrocarbons. *Prog. Energy Combust. Sci.* **1986**, *12* (1), 1−24.
(25) Taatjes, C. A.; Osborn, D. L.; Selby, T. M.; Meloni, G.; Trevitt, A. J.; Epifanovsky, E.; Krylov, A. I.; Sirjean, B.; Dames, E.; Wang, H. Products of the Benzene + O(^{3}P) Reaction. *J. Phys. Chem. A* **2010**, *114* (9), 3355−3370.
(26) Zhao, L.; Yang, T.; Kaiser, R. I.; Troy, T. P.; Xu, B.; Ahmed, M.; Alarcon, J.; Belisario-Lara, D.; Mebel, A. M.; Zhang, Y.; et al. A Vacuum Ultraviolet Photoionization Study on High-Temperature Decomposition of JP-10 (: Exo -Tetrahydrodicyclopentadiene). *Phys. Chem. Chem. Phys.* **2017**, *19* (24), 15780−15807.
(27) Striebich, R. C.; Lawrence, J. Thermal Decomposition of High-Energy Density Materials at High Pressure and Temperature. *J. Anal. Appl. Pyrolysis* **2003**, *70* (2), 339−352.
(28) Magoon, G. R.; Yee, N. W.; Oluwole, O. O.; Bonomi, R. E.; Wong, H.-W.; Van Geem, K. M.; Lewis, D. K.; Green, W. H.; Vandewiele, N. M.; Gao, C. W.; et al. JP-10 Combustion Studied with Shock Tube Experiments and Modeled with Automatic Reaction Mechanism Generation. *Combust. Flame* **2015**, *162* (8), 3115−3129.
(29) Nageswara Rao, P.; Kunzru, D. Thermal Cracking of JP-10: Kinetics and Product Distribution. *J. Anal. Appl. Pyrolysis* **2006**, *76* (1−2), 154−160.
(30) Xing, Y.; et al. Thermal Cracking of JP-10 under Pressure. *Ind. Eng. Chem. Res.* **2008**, *47* (24), 10034−10040.
(31) Wang, D.; Violi, A.; Kim, D. H.; Mullholland, J. A. Formation of Naphthalene, Indene, and Benzene from Cyclopentadiene Pyrolysis: A DFT Study. *J. Phys. Chem. A* **2006**, *110* (14), 4719−4725.
(32) Violi, A.; Sarofim, A. F.; Truong, T. N. Quantum Mechanical Study of Molecular Weight Growth Process by Combination of Aromatic Molecules. *Combust. Flame* **2001**, *126*, 1506−1515.
(33) Violi, A. Cyclodehydrogenation Reactions to Cyclopentafused Polycyclic Aromatic Hydrocarbons. *J. Phys. Chem. A* **2005**, *109*, 7781−7787.
(34) D'Anna, A.; Violi, A. Detailed Modeling of the Molecular Growth Process in Aromatic and Aliphatic Premixed Flames. *Energy Fuels* **2005**, *19* (1), 79−86.
(35) Trevitt, A. J.; Goulay, F. Insights into Gas-Phase Reaction Mechanisms of Small Carbon Radicals Using Isomer-Resolved Product Detection. *Phys. Chem. Chem. Phys.* **2016**, *18* (8), 5867−5882.
(36) Goulay, F.; Trevitt, A. J.; Meloni, G.; Selby, T. M.; Osborn, D. L.; Taatjes, C. A.; Vereecken, L.; Leone, S. R. Cyclic versus Linear Isomers Produced by Reaction of the Methylidyne Radical (CH) with Small Unsaturated Hydrocarbons. *J. Am. Chem. Soc.* **2009**, *131* (3), 993−1005.
(37) Hughes, K. J.; McKee, K.; Blitz, M. A.; Pilling, M. J.; Taylor, A.; Qian, H.-B.; Seakins, P. W. H Atom Branching Ratios from the Reactions of CH with C_2H_2, C_2H_4, C_2H_6, and Neo-C_5H_{12} at Room Temperature and 25 Torr. *J. Phys. Chem. A* **2003**, *107* (30), 5710−5716.
(38) Loison, J. C.; Bergeat, A.; Caralp, F.; Hannachi, Y. Rate Constants and H Atom Branching Ratios of the Gas-Phase Reactions of Methylidyne CH($X^2\Pi$) Radical with a Series of Alkanes. *J. Phys. Chem. A* **2006**, *110* (50), 13500−13506.
(39) Fleurat-Lessard, P.; Rayez, J. C.; Bergeat, A.; Loison, J. C. Reaction of Methylidyne CH($X^2\Pi$) Radical with CH_4 and H_2S: Overall Rate Constant and Absolute Atomic Hydrogen Production. *Chem. Phys.* **2002**, *279* (2−3), 87−99.
(40) Canosa, A.; Sims, I. R.; Travers, D.; Smith, I. W. M.; Rowe, B. R. Reactions of the Methylidine Radical with CH_4, C_2H_2, C_2H_4, C_2H_6, and but-1-Ene Studied between 23 and 295 K with a CRESU Apparatus. *Astron. Astrophys.* **1997**, *323*, 644−651.
(41) Daugey, N.; Caubet, P.; Retail, B.; Costes, M.; Bergeat, A.; Dorthe, G. Kinetic Measurements on Methylidyne Radical Reactions with Several Hydrocarbons at Low Temperatures. *Phys. Chem. Chem. Phys.* **2005**, *7* (15), 2921−2927.
(42) Thiesemann, H.; MacNamara, J.; Taatjes, C. A. Deuterium Kinetic Isotope Effect and Temperature Dependence in the Reactions of CH with Methane and Acetylene. *J. Phys. Chem. A* **1997**, *101* (10), 1881−1886.
(43) Soorkia, S.; Taatjes, C. A.; Osborn, D. L.; Selby, T. M.; Trevitt, A. J.; Wilson, K. R.; Leone, S. R. Direct Detection of Pyridine Formation by the Reaction of CH (CD) with Pyrrole: A Ring Expansion Reaction. *Phys. Chem. Chem. Phys.* **2010**, *12* (31), 8750−8758.
(44) Maksyutenko, P.; Zhang, F.; Gu, X.; Kaiser, R. I. A Crossed Molecular Beam Study on the Reaction of Methylidyne Radicals [CH($X^2\Pi$)] with Acetylene [C_2H_2 ($X^1\Sigma_g^+$)]—Competing C_3H_2 + H and C_3H + H. *Phys. Chem. Chem. Phys.* **2011**, *13* (1), 240−252.
(45) Berman, M. R.; Fleming, J. W.; Harvey, A. B.; Lin, M. C. Temperature Dependence of the Reactions of CH Radicals with Unsaturated Hydrocarbons. *Chem. Phys.* **1982**, *73*, 27−33.
(46) Butler, J. E.; Fleming, J. W.; Goss, L. P.; Lin, M. C. Kinetics of CH Radical Reactions with Selected Molecules at Room Temperature. *Chem. Phys.* **1981**, *56* (3), 355−365.
(47) Trevitt, A. J.; Prendergast, M. B.; Goulay, F.; Savee, J. D.; Osborn, D. L.; Taatjes, C. A.; Leone, S. R. Product Branching Fractions of the CH + Propene Reaction from Synchrotron Photoionization Mass Spectrometry. *J. Phys. Chem. A* **2013**, *117* (30), 6450−6457.
(48) Ribeiro, J. M.; Mebel, A. M. Reaction Mechanism and Product Branching Ratios of the CH + C_3H_8 Reaction: A Theoretical Study. *J. Phys. Chem. A* **2014**, *118* (39), 9080−9086.
(49) Butler, J. E.; Fleming, J. W.; Goss, L. P.; Lin, M. C. Kinetics of CH Radical Reactions Important to Hydrocarbon Combustion Systems. *Laser Probes Combust. Chem.* **1980**, *134*, 397−401.
(50) Goulay, F.; Rebrion-Rowe, C.; Biennier, L.; Le Picard, S. D.; Canosa, A.; Rowe, B. R. Reaction of Anthracene with CH Radicals: An Experimental Study of the Kinetics between 58 and 470 K. *J. Phys. Chem. A* **2006**, *110* (9), 3132−3137.
(51) Madden, L. K.; Mebel, A. M.; Lin, M. C.; Melius, C. F. Theoretical Study of the Thermal Isomerization of Fulvene to Benzene. *J. Phys. Org. Chem.* **1996**, *9* (12), 801−810.
(52) Jasper, A. W.; Hansen, N. Hydrogen-Assisted Isomerizations of Fulvene to Benzene and of Larger Cyclic Aromatic Hydrocarbons. *Proc. Combust. Inst.* **2013**, *34*, 279−287.
(53) Abhinavam Kailasanathan, R. K.; Thapa, J.; Goulay, F. Kinetic Study of the OH Radical Reaction with Phenylacetylene. *J. Phys. Chem. A* **2014**, *118* (36), 7732−7741.
(54) Herbert, L. B.; Sims, I. R.; Smith, I. W. M.; Stewart, D. W. A.; Symonds, A. C.; Canosa, A.; Rowe, B. R. Rate Constants for the Relaxation of CH($X^2\Pi$) by CO and N_2 at Temperatures from 23 to 584 K. *J. Phys. Chem.* **1996**, *100* (36), 14928−14935.
(55) Liu, W.-L.; Chang, B.-C. Transient Frequency Modulation Spectroscopy and 266nm Photodissociation of Bromoform. *J. Chin. Chem. Soc.* **2001**, *48*, 613−617.
(56) Zou, P.; Shu, J.; Sears, T. J.; Hall, G. E.; North, S. W. Photodissociation of Bromoform at 248nm: Single and Multiphoton Processes. *J. Phys. Chem. A* **2004**, *108*, 1482−1488.
(57) Moffett, R. B. Cyclopentadiene and 3-Chlorocyclopentene. *Org. Synth.* **1952**, *32*, 41−44.
(58) Gallinella, E.; Fortunato, B.; Mirone, P. Infrared and Raman Spectra and Vibrational Assignment of Cyclopentadiene. *J. Mol. Spectrosc.* **1967**, *24*, 345−362.
(59) Frisch, M. J.; Trucks, G. W.; Schlegel, H. B.; Scuseria, G. E.; Robb, M. A.; Cheeseman, J. R.; Scalmani, G. *Gaussian 09*; Gaussian, Inc.: Wallingford, CT, 2016.
(60) Becke, A. D. A New Mixing of Hartree-Fock and Local Density-Functional Theories. *J. Chem. Phys.* **1993**, *98* (2), 1372−1377.
(61) Somers, K. P.; Simmie, J. M. Benchmarking Compound Methods (CBS-QB3, CBS-APNO, G3, G4, W1BD) against the Active Thermochemical Tables: Formation Enthalpies of Radicals. *J. Phys. Chem. A* **2015**, *119* (33), 8922−8933.

DOI: 10.1021/acs.jpca.9b03813
J. Phys. Chem. A 2019, 123, 5692−5703

(62) Montgomery, J. A.; Frisch, M. J.; Ochterski, J. W.; Petersson, G. A. A Complete Basis Set Model Chemistry. VII. Use of Density Functional Geometries and Frequencies. *J. Chem. Phys.* **1999**, *110* (6), 2822−2827.
(63) Montgomery, J. A.; Frisch, M. J.; Ochterski, J. W.; Petersson, G. A. A Complete Basis Set Model Chemistry. VII. Use of the Minimum Population Localization Method. *J. Chem. Phys.* **2000**, *112* (15), 6532−6542.
(64) Zabarnick, S.; Fleming, J. W.; Lin, M. C. Kinetics of CH Radical Reactions with Propane, Isobutane and Neopentane. *Chem. Phys.* **1987**, *112*, 409−413.
(65) Thiesemann, H.; Clifford, E. P.; Taatjes, C.; Klippenstein, S. J. Temperature Dependence and Deuterium Kinetic Isotope Effects in the CH (CD) + C_2H_4 (C_2D_4) Reaction between 295 and 726 K. *J. Phys. Chem. A* **2001**, *105* (22), 5393−5401.
(66) Thapa, J.; Spencer, M.; Akhmedov, N. G.; Goulay, F. Kinetics of the OH Radical Reaction with Fulvenallene from 298 to 450 K. *J. Phys. Chem. Lett.* **2015**, *6* (24), 4997−5001.
(67) Powell, J. S.; Edson, K. C. Spectroscopic Determination of Cyclopentadiene and Methylcyclopentadiene. *Anal. Chem.* **1948**, *20* (6), 510−511.
(68) Melius, C.; Colvin, M.; Marinov, N.; Pitz, W.; Senkan, S. Reaction Mechanisms in Aromatic Hydrocarbon Formation Involving the C_5H_5 Cyclopentadienyl Moiety. *Symp. (Int.) Combust., [Proc.]* **1996**, *26* (1), 685−692.
(69) Bergeat, A.; Loison, J.-C. Reaction of Carbon Atoms, C ($2p^2$, ^3P) with C_2H_2, C_2H_4 and C_6H_6: Overall Rate Contant and Relative Atomic Hydrogen Production. *Phys. Chem. Chem. Phys.* **2001**, 3, 2038−2042.
(70) Stoecklin, T.; Dateo, C. E.; Clary, D. C. Rate Constant Calculations on Fast Diatom-Diatom Reactions. *J. Chem. Soc., Faraday Trans.* **1991**, *87* (11), 1667−1679.
(71) Clary, D. Fast Chemical Reactions: Theory Challenges Experiment. *Annu. Rev. Phys. Chem.* **1990**, *41* (1), 61−90.
(72) Ribeiro, J. M.; Mebel, A. M. Reaction Mechanism and Product Branching Ratios of the CH + C_3H_6 Reaction: A Theoretical Study. *J. Phys. Chem. A* **2016**, *120*, 1800−1812.
(73) Zhang, F.; Maksyutenko, P.; Kaiser, R. I. Chemical Dynamics of the CH($X^2\Pi$) + C_2H_4($X^1A^1_g$), CH($X^2\Pi$) + C_2D_4($X^1A^1_g$), and CD($X^2\Pi$) + C_2H_4. *Phys. Chem. Chem. Phys.* **2012**, *14* (2), 529−537.
(74) Vereecken, L.; Pierloot, K.; Peeters, J. B3LYP-DFT Characterisation of the Potential Energy Surface of the CH($X^2\Pi$) + C_2H_2 Reaction. *J. Chem. Phys.* **1998**, *108* (3), 1068−1080.
(75) Jones, B. M.; Zhang, F.; Kaiser, R. I.; Jamal, A.; Mebel, A. M.; Cordiner, M. A.; Charnley, S. B. Formation of Benzene in the Interstellar Medium. *Proc. Natl. Acad. Sci. U. S. A.* **2011**, *108* (2), 452−457.
(76) Dubnikova, F.; Lifshitz, A. Ring Expansion in Methylcyclopentadiene Radicals. Quantum Chemical and Kinetics Calculations. *J. Phys. Chem. A* **2002**, *106* (35), 8173−8183.
(77) Sharma, S.; Harper, M. R.; Green, W. H. Modeling of 1,3-Hexadiene, 2,4-Hexadiene and 1,4-Hexadiene-Doped Methane Flames: Flame Modeling, Benzene and Styrene Formation. *Combust. Flame* **2010**, *157* (7), 1331−1345.
(78) Krasnoukhov, V. S.; Porfiriev, D. P.; Zavershinskiy, I. P.; Azyazov, V. N.; Mebel, A. M. Kinetics of the CH_3 + C_5H_5 Reaction: A Theoretical Study. *J. Phys. Chem. A* **2017**, *121* (48), 9191−9200.
(79) Loison, J.-C.; Bergeat, A. Rate Constants and the H Atom Branching Ratio of the Reactions of the Methylidyne CH($X^2\Pi$) Radical with C_2H_2, C_2H_4, C_3H_4, C_3H_6 and C_4H_8. *Phys. Chem. Chem. Phys.* **2009**, *11* (4), 655−664.
(80) Galland, N.; Caralp, F.; Hannachi, Y.; Bergeat, A.; Loison, J. C. Experimental and Theoretical Studies of the Methylidyne Radical Reaction with Ethane (C_2H_6): Overall Rate Constant and Product Channels. *J. Phys. Chem. A* **2003**, *107* (28), 5419−5426.
(81) Tang, W.; Tranter, R. S.; Brezinsky, K. An Optimized Semidetailed Submechanism of Benzene Formation from Propargyl Recombination. *J. Phys. Chem. A* **2006**, *110* (6), 2165−2175.
(82) Tang, W.; Tranter, R. S.; Brezinsky, K. Isomeric Product Distributions from the Self-Reaction of Propargyl Radicals. *J. Phys. Chem. A* **2005**, *109* (27), 6056−6065.
(83) Fitzpatrick, E. M.; Jones, J. M.; Pourkashanian, M.; Ross, A. B.; Williams, A.; Bartle, K. D. Mechanistic Aspects of Soot Formation from the Combustion of Pine Wood. *Energy Fuels* **2008**, *22* (6), 3771−3778.
(84) Daniel, R.; Wei, L.; Xu, H.; Wang, C.; Wyszynski, M. L.; Shuai, S. Speciation of Hydrocarbon and Carbonyl Emissions of 2,5-Dimethylfuran Combustion in a DISI Engine. *Energy Fuels* **2012**, *26* (11), 6661−6668.
(85) Jia, X.; Guo, B.; Jin, B.; Zhang, X.; Jing, K.; Liu, G. High-Pressure Thermal Decomposition of Tetrahydrotricyclopentadiene (THTCPD) and Binary High-Density Hydrocarbon Fuels of JP-10/THTCPD in a Tubular Flowing Reactor. *Energy Fuels* **2017**, *31* (8), 8023−8035.
(86) Guo, B.; Wang, Y.; Wang, L.; Zhang, X.; Liu, G. Thermal Decomposition and Kinetics of a High-Energy-Density Hydrocarbon Fuel: Tetrahydrotricyclopentadiene (THTCPD). *Energy Fuels* **2016**, *30* (1), 230−238.
(87) Moskaleva, L. V.; Mebel, A. M.; Lin, M. C. The CH_3 + C_5H_5 Reaction: A Potential Source of Benzene at High Temperatures. *Symp. Combust., [Proc.]* **1996**, *26* (1), 521−526.
(88) Sharma, S.; Green, W. H. Computed Rate Coefficients and Product Yields for C_5H_5 + CH_3. *J. Phys. Chem. A* **2009**, *113*, 8871−8882.

DOI: 10.1021/acs.jpca.9b03813
J. Phys. Chem. A 2019, 123, 5692−5703